Research Article

Journal of PeptideScience

Received: 27 June 2008 Revised: 22 September 2008 Accepted: 24 September 2008 Published online in Wiley Interscience: 20 November 2008

(www.interscience.com) DOI 10.1002/psc.1083

# Self-assembling properties of ionic-complementary peptides‡

**Gabriella D'Auria,[a,b]* Manuela Vacatello,[a] Lucia Falcigno,[a,b] Luigi Paduano,[a,c] Gaetano Mangiapia,[a,c] Luisa Calvanese,[a] Roberta Gambaretto,[d] Monica Dettin[d] and Livio Paolillo[a,b]**

**Self-complementary synthetic peptides, composed by 8 and 16 residues, were analyzed by CD, NMR and small angle neutron scattering (SANS) techniques in order to investigate the relevance of charge and hydrophobic interactions in determining their self-assembling properties. All the sequences are potentially able to form fibrils and membranes as they share, with the prototype EAK16, a strictly alternating arrangement of polar and nonpolar residues. We find that 16-mer peptides show higher self-assembling propensities than the 8-mer analogs and that the aggregation processes are favored by salts and neutral pH. Peptide hydrophobic character appears as the most relevant factor in determining self-assembling. Solution conformational analysis, diffusion and SANS measurements all together show that the sequences with a higher self-assemble propensity are distributed, in mild conditions, between light and heavy forms. For some of the systems, the light form is mostly constituted by monomers in a random conformation, while the heavy one is constituted by $\beta$-aggregates. In our study we also verified that sequences designed to adopt extended conformation, when dissolved in alcohol-water mixtures, can easily fold in helix structures. In that media, the prototype of the series appears distributed between helical monomers and $\beta$-aggregates. It is worth noticing that the structural conversion from helical monomer to $\beta$-aggregates, mimics $\beta$-amyloid peptide aggregation mechanisms.** 

*Supporting information may be found in the online version of this article*

**Keywords:** self-assembling; $\beta$-propensity; SANS; diffusion; PFGNMR; bio-membrane; EAK16-II analogs; amyloidosis

## Introduction

Molecular self-assembling, i.e. the spontaneous organization of molecules under thermodynamic equilibrium conditions into structurally well-defined arrangements [1], is a very functional process in biological systems. In the past decade, a lot of attention was focused on protein and peptide self-assembling mechanisms. Indeed, the understanding of the molecular details of the process is a challenging objective in the perspective of controlling protein aggregation related pathologies [2], as well as to exploit peptides self-assembling for nano-technological purposes, for example, in the development of new biomaterials for tissue engineering [3,4].

A class of peptides with self-assembling characteristics is that of the ionic-complementary peptides. Their potential applications in bionanotechnology were firstly proposed by Zhang *et al*. in 1993 [5,6]. These peptides are characterized by an alternating arrangement of hydrophobic and hydrophilic amino acid residues that imparts to them an amphiphilic property. The secondary structure they will adopt in the assembling is due to how the hydrophobic and the hydrophilic residues are positioned along the sequence. If they have a periodicity • • − − • • + + (where • is a hydrophobic residue, − is an acid residue and + is a basic amino acid) they will assemble through helical-structures; if they have a periodicity • − • +, i.e. alternated, they will assemble into a $\beta$-structure. As Hecht and his group have demonstrated [7], this happens because the amino acid intrinsic propensity for secondary structure is overwhelmed by the drive to form amphiphilic structures capable of burying a hydrophobic surface area. The first member of the ionic-complementary peptide family discovered by Zhang *et al*. is EAK16-II (Table 1). This sequence, a 16-mer composed by repetition of a self-complementary octa-peptide, forms beta-sheets in pure water and, in the presence of monovalent cation salts, grows into a microscopic ordered membrane. The hypothesized mechanism for the formation of the membrane is first the assembly of the peptide monomers into beta-sheets through hydrogen-bonds, and then the stacking of the so-formed amphiphilic sheets through an alternation of ionic and hydrophobic interactions [5]. Furthermore, a self-assembly model for the EAK16-II fibril formation was recently reported by Fung *et al*. [8]. According to Hecht's statement [7], Zhang hypothesized that,

* *Correspondence to: Gabriella D'Auria, Dipartimento di Chimica, Università degli Studi di Napoli "Federico II", via Cintia, 45, 80126, Napoli, Italy. E-mail: gabriella.dauria@unina.it*

a *Department of Chemistry, University of Naples "Federico II", 80126 Naples, Italy*

b *Institute of Biostructures and Bioimaging, CNR, 80134 Naples, Italy*

c *Consorzio per lo sviluppo dei Sistemi a Grande Interfase (CSGI), Italy*

d *Department of Chemical Process Engineering, University of Padua, 35131 Padua, Italy*

‡ *11th Naples Workshop on Bioactive Peptides.*

 

if substitution of the charged residues of EAK16-II sequence with other similarly charged amino acids or substitution of hydrophobic residues with other hydrophobic amino acids occurs, no drastic effects are to be observed on the self-assembly process. In this work, some analogs of the EAK16-II peptide were synthesized in order to study, by using NMR and small angle neutron scattering (SANS) methodologies, the role of different residues in inducing the beta-sheet structure. The modifications of the model sequence (EAK16-II, in the following renamed EAK16) were conservative in comparison with polar/nonpolar periodicity: Glu → Asp in DAK16; Glu → Asp and Lys → Orn in DAOrn16; Ala → Abu in EAbuK16; Ala → Tyr in EYK16 (Table 1). Furthermore, for its potential application as building block of biocompatible membrane useful in tissue engineering, the conformational and aggregative behavior of RGD-EAK16 was also studied. One of the possible scrambled analog of this last sequence, RGD-EAK16-Sc, completely lacking any structure periodicity, was also included as an element of comparison (Table 1). Finally the shorter sequences composed by a single self-complementary 8 residues module, EAK8, EAbuK8, DAK8, DAOrn8 and EYK8 were analyzed (Table 2).

Recently, the conformational studies on our 16-mer peptides by CD [9] and IR/Raman spectroscopy [10] were reported. Here the solution NMR analysis of all the peptides and also the CD analysis of the 8-mer series are presented. Different conditions were explored in the attempt to stabilize some early stages of aggregation. Furthermore, to characterize the dimension of the molecular systems in solution, diffusion ordered spectroscopy by Pulse Field Gradient Technique (PFGNMR) and SANS experiments were performed.

## Materials and Methods

All the peptides analyzed in this work were synthesized and purified as reported in Ref. 9.

### CD Analysis

CD spectra were obtained on a Jasco J-710 model spectropolarimeter. Data were elaborated using J-700 software supplied by Jasco (Tokyo, Japan). Measurements were performed on 50 μM peptide 2,2,2-TFE or water solutions. The TFE solution was prepared by dissolving a weighted quantity of peptide in the minimum amount of water to which TFE was added giving a final content of 98% (v/v). Samples were analyzed at room temperature (RT) in cylindrical fused quartz cuvettes with a 0.1 cm path length and in the 185–250-nm wavelength range, averaged for 2–4 scans. Data points were recorded at a scan speed of 5 or 20 nm/min, bandwidth of 2.0 nm, 2-s response and 0.2-nm resolution. After baseline correction, CD spectra were normalized using the exact peptide concentration obtained from quantitative amino acid analysis. The spectra are reported in mean residue ellipticity (deg $cm^2$ $dmol^{-1}$).

### NMR Analysis

NMR experiments were carried out on an INCA (Consorzio Interuniversitario Chimica per l'Ambiente) Varian Inova 500 MHz, located at the 'Centro Interdipartimentale di Metodologie Chimico Fisiche', Università 'Federico II' di Napoli, Italy. NMR characterization was performed in $H_2O/D_2O$ 90/10 (v/v) prepared using pure $H_2O$ or NaCl solutions at salt concentrations of 30 and 100 mM, and

**Table 1.** Sequences of the 16-mer peptides, secondary structure diagnoses by CD and NMR analyses and estimation of the self-aggregation abilities in solution

| Nick-name of 16-mer analogs | Modification | Sequence | m.h.m[a] | Structure in $H_2O$ by CD [9]/NMR | Self-aggreg. in $H_2O$ mild condition: yes or no | Structure in TFE/$H_2O$ by CD [9]/NMR[b] | Self-aggreg. in TFE/$H_2O$: yes or no |
|---|---|---|---|---|---|---|---|
| EAK16 | Prototype | $(AEAEAKAK)_2$ | 4.02 | $\beta^+$/r | Yes | $\beta/\alpha^+$ | Yes |
| EAbuK16 | Ala → Abu | $(AbuEAbuEAbuKAbuK)_2$ | 5.42 | $\beta^{++}/-$ | Yes+ | $\beta/\alpha$ | Yes |
| RGD-EAK16 | Arg-Gly-Asp addition | $RGD(AEAEAKAK)_2$ | 4.22 | $\beta$/r | Yes | $\beta$/n.a. | n.a |
| DAK16 | Glu → Asp | $(ADADAKAK)_2$ | 4.02 | $\alpha$(32%)/r | No | $\alpha$/n.a. | n.a |
| DAOrn16 | Lys → Orn, Glu → Asp | $(ADADAOrnAOrn)_2$ | 3.77 | $\alpha$(36%)/r | No | $\alpha$/n.a. | n.a |
| RGD-EAK16-Sc | RGD+EAK16-scrambled | RGD-AAKA-EAEA-AEKA-KAEK | 1.11 | $\alpha$(40%)/r | No | $\alpha/\alpha$ | No |
| EYK16 | Ala → Tyr | $(YEYEYKYK)_2$ | 5.82 | hairpin | Yes | n.a. | n.a |

[a] m.h.m: mean hydrophobic moment calculated via HydroMCalc (by Alex Tossi and Luca Sandri.:http://www.bbcm.univ.trieste.it/~tossi/HydroCalc/HydroMCalc.html) by assuming the peptides in extended conformation.
[b] n.a., not analyzed.

**Table 2.** Sequences of the 8-mer peptides, secondary structure diagnoses by CD and NMR analyses and estimation of the self-aggregation abilities in solution

| Nick-name of 8-mer | Modification | Sequence | m.h.m. | Structure in $H_2O$ by CD/NMR | Self-aggreg. in $H_2O$ (all conditions) |
|---|---|---|---|---|---|
| EAK 8 | Prototype | AEAEAKAK | 4.02 | r/r | No |
| EAbuK 8 | Ala → Abu | AbuEAbuEAbuKAbuK | 5.42 | r/propensity to extended conformation | No |
| DAK 8 | Glu → Asp | ADADAKAK | 4.02 | r/r | No |
| DAOrn 8 | Lys → Orn, Glu → Asp | ADADAOrnAOrn | 3.77 | r/r | No |
| EYK8 | Ala → Tyr | YEYEYKYK | 5.82 | r/propensity to extended conformation | No |

  

in trifluoroethanol TFE/$H_2O$ 30:70 (v/v) at 298 K. Samples were prepared by dissolving weighted amounts of peptides in 600 µl of solvent mixture $H_2O/D_2O$ 90/10 (v/v), or NaCl solutions/$D_2O$ 90/10 (v/v) or TFE/$H_2O$ 30:70 (v/v) for final concentrations of 1–3 mM. The spectra measured in water were acquired in the pH range 3.4–6. Chemical shifts were referenced to internal sodium 3-(trimethylsilyl)[2,2′,3,3′-$d_4$] propionate (TSP). For EAK16 sample, the effective peptide concentration observed by NMR was checked by using L-Tryptophan methyl ester hydrochloride (from Aldrich, code 36,451-7) as internal reference. The check was performed by integrating well-isolated signals (Ala$^1$-$\alpha$CH at 4.09 ppm and Trp-$\beta\beta'CH_2$ at 3.48 ppm) in 1D spectra acquired with a recycle time of 3.6 s.

Two dimensional experiments, TOCSY, NOESY, ROESY, double-quantum-filtered correlation spectroscopy (DQFCOSY) were measured with standard pulse sequences [11–15]. Typically, the water resonance was suppressed by low-power selective irradiation during the relaxation delay. Sequential assignment was achieved according to Wüthrich [16], NOE/rotating-frame overhauser enhancement (ROE) analysis was achieved by means of NOESY/ROESY spectra, acquired with 100 and 200 ms mixing times. NOE/ROE cross-peaks were integrated with NMR view [17] and then converted into upper-distance bounds with routine CALIBA of the package DYANA [18]. Geminal protons, not stereospecifically assigned, were substituted by pseudo atoms [19].

### Computational Analysis

Molecular models of EAK16 in TFE/$H_2O$ 30/70 (v:v) were calculated by the DYANA program [18] using 75 NOE interproton distances (37 intra, 34 sequential, 4 long range) as upper limits. Additional constraints were used for $\phi$ dihedral angles of those residues showing values of $^3J_{NH-\alpha CH} < 5$ Hz [20]. In those cases $\phi$ angles were set to $-57^\circ$ with a tolerance $\pm 10^\circ$ for residues with $^3J_{NH-\alpha CH} < 4$ Hz, and with a tolerance of $\pm 20^\circ$ for residues where $4\text{ Hz} < {}^3J_{NH-\alpha CH} < 5$ Hz.

A first set of 40 conformers was calculated with the standard parameters of the DYANA program, and 100 additional structures were calculated using the redundant dihedral angle constraints (REDAC) strategy [21] on five cycles to improve the convergence. The final 100 structures calculated show an average target function (TF) value of $0.17 \pm 6.6\text{E}{-}02$ Å$^2$ and a mean global backbone root mean square deviation (RMSD) of $1.62 \pm 0.58$ Å. The 30 DYANA structures for peptide EAK16 (analyzed in TFE/$H_2O$ 30/70) with the lowest values of the TF were subjected to restrained energy minimization using the SANDER module of the AMBER 6.0 package [22]. The molecular graphics program MOLMOL [23] was employed to perform the structural statistics analysis. The best 10 structures, in terms of fitting with the experimental restraints among those with a residual energy lower than $-118.45$ Kcal mol$^{-1}$, were chosen to represent the conformational behavior of peptide EAK16 in TFE/$H_2O$ 30/70.

Molecular models of EAbuK8 and EYK8 in water ($H_2O/D_2O$ 90/10 v : v) were calculated by DYANA program using a set of 50 (33 intraresidue, 17 sequential) and 55 (40 intraresidue, 15 sequential) experimental NOE constraints, respectively. The final 100 structures, generated for each peptide, show an average TF of $6.0\text{E}{-}02 \pm 2.0\text{E}{-}02$ Å$^2$ and $7.7\text{E}{-}02 \pm 2.1\text{E}{-}02$ Å$^2$ a mean global backbone RMSD of $2.07 \pm 0.51$ Å and $1.39 \pm 0.44$ Å, respectively. More details on structure calculations are reported as Supporting Information.

### NMR Diffusion Experiment

Pulsed field gradient nuclear magnetic resonance (PFGNMR) spectra were acquired at 298 K on a Varian Inova 500 spectrometer equipped with a Performa II gradient pulse amplifier and an actively shielded 5-mm indirect detection probe (Dipartimento di Scienze Ambientali, Seconda Università di Napoli, Caserta, Italy). A bipolar pulse pair stimulated echo sequence with Watergate suppression was used [24]. The gradient strength was calibrated using proton signal in 1% $H_2O$ in a $D_2O$ sample and a literature value of $1.90 \times 10^{-9}$ m$^2$ s$^{-1}$ for the HDO translational diffusion coefficient. Diffusion coefficients were measured by incrementing the amplitude of the field gradient pulses in a square fashion from an initial value of ~1 G/cm to a final value of ~60 G/cm, while the duration (2 ms), the separation (100 ms) of the field gradients and the total echo time were kept constant. Typically, a series of 16 spectra with 64 scans were recorded.

For a single diffusing species, the signal attenuation in the presence of a pair of bipolar-pulsed field gradients is given by

$$I = I_0 \exp(-\gamma^2 g^2 D\delta^2(\Delta - \delta/3 - \tau/2) \quad (1)$$

where $\gamma$ is the gyromagnetic ratio, $g$, $\delta$ and $\Delta$ are the amplitude, duration and separation of the pair of bipolar gradient pulses and $\tau$ is the separation between the gradients within each bipolar gradient pulse [24]. The translational diffusion coefficients $D_t$ were obtained by fitting Eqn (1) to the peak intensities. The oligomerization state of the peptides whose $D_t$ coefficients we measured in water at 25 °C, was estimated by comparison with experimental $D_t$ values reported by Danielsson on a series of random coil $\beta$-amyloid analogs in the same solvent and temperature [25]. We performed a linear regression ($y = 3\text{E} + 08x + 0.022$) between the inverse cubic root of the molecular weights, $(\text{MW})^{-1/3}$, and $D_t$ coefficients in Danielsson [25] with a very good coefficient $R^2$ of 0.995. The molecular masses estimated by fitting our $D_t$ values to the curve obtained by the Danielsson data indicate that the peptide systems, which give rise to the NMR spectra, are predominantly monomeric in solution. The oligomerization state of the peptides whose $D_t$ coefficients we measured in TFE/$H_2O$ 30/70 was determined by fitting our data to a linear correlation, $(\text{MW})^{-1/3}$ *vs* $D_t$, based on diffusion data of standard molecules in the same solvent mixture (TSP, $MW = 150.03$ Da, $D_t = 3.45 \times 10^{-10}$ m$^2$ s$^{-1}$; synthetic monomeric peptide, $MW = 2111.43$ Da, $D_t = 1.12 \times 10^{-10}$ m$^2$ s$^{-1}$).

### SANS Measurements

SANS measurements were performed at 25 °C using the PAXE spectrometer located at the Laboratoire Léon Brillouin (Saclay, France). Neutrons with an average wavelength $\lambda$ of 8 Å and a wavelength spread $\Delta\lambda/\lambda < 15\%$ were used. Neutrons scattered from the sample were detected by a two dimensional array detector sited at two different sample-to-detector distances (1.3 and 5.0 m). These configurations allowed collecting the scattered neutrons in a range of transferred momentum $q$ between 0.005 and 0.21 Å$^{-1}$. Samples, prepared by weight using $D_2O$ as solvent, were contained in 1 mm path length quartz cells and measurement times ranged between 20 min and 2 h. The data were then corrected for background, empty cell and solvent contribution, and then reduced to scattering cross sections (in absolute units cm$^{-1}$), following the standard procedure [26,27].

  

## Results

### 16-mer Analogs

The main results of the recently reported CD analyses of the 16-mer analogs [9] are summarized in Table 1. Generally, the peptides with the higher hydrophobic moments exhibit higher rates of $\beta$-structure. Indeed, while the prototype EAK16, RGD-EAK16 and EAbuK16 are found in a predominantly beta-sheet form, the less hydrophobic peptides of the series, DAOrn16 and RGD-EAK-Sc, show preference for a $\alpha$-helix structure. However, an easy correlation between hydrophobicity and $\beta$-propensity does not seem straightforward. EYK16, the most hydrophobic peptide of the series, is found in a $\beta$-hairpin structure while the peptide DAK16, with the same mean hydrophobic moment of EAK16, fails to arrange into a $\beta$-structure and shows, instead, a 32% helix content [9].

Quite surprisingly, the NMR analysis performed on all the 16-mer sequences drives to structural diagnoses apparently different from those obtained by the CD analyses performed at identical peptide concentrations and solvent conditions [9]. To the NMR reading, all the peptides of the series appear random in water solution. In particular, no long-range NOE effects and few $NH_i-NH_{i+1}$ are detected. Furthermore, not rarely the intraresidue $NH_i-\alpha CH_i$ and sequential $\alpha CH_i-NH_{i+1}$ NOE effects are superimposed with each other as a consequence of the small distributions of the $\alpha$CH chemical shifts. Globally, conformational disorder is easily diagnosed by the lack of any NOE pattern canonical for secondary structure and also by the chemical shift values measured for the $\alpha$CH protons of the amino acids (Figure 1), typical for residues in a random conformation [28]. The behavior of the 16-mer peptides in water was monitored with time, pH, peptide concentration and metal ion. The effects produced on the peptides spectra by changing those parameters one at a time, are shortly summarized in the following. We anticipate here that, under no conditions, the NMR technique evidenced the presence of ordered systems.

*Time effect*

The different sequences in the identical mild conditions (0.7–1 mM, pH 3.3–3.8) show different behavior with time. The NMR spectra of the most hydrophobic peptide of the series, EYK16, vanish in weeks (Fig. S1a,b of the Supporting Information). EAbuK16, the second sequence in the hydrophobicity rank, shows spectra very reproducible in time but characterized by very low and broad signals (Fig. S1c,d of Supporting Information). Indeed, the extensive self-aggregation makes EAbuK16 apparently well soluble at millimolar concentrations, unfit for the NMR analysis. All the other sequences of the series (for 1D spectra see Fig. S2 of Supporting Information) show, at acidic pH and without salts, NMR spectra very reproducible in time. The 1D spectra acquired at two different times for EAK16 in water and in presence of L-Tryptophan methyl ester as internal standard are reported in Figure 2. After 5 months (Figure 2(b)) since the sample preparation (Figure 2(a)),

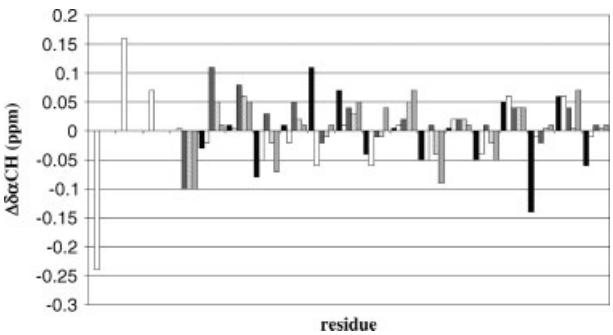


**Figure 1.** Chemical shift deviations from random coil values of $\alpha$CH protons ($\Delta\delta_{\alpha CH}$) of the 16-mer analogs 1 mM in water: EYK16 (black), EAK16 (dark gray), RGD-EAK16 (white) DAK16 (dashed), DAOrn16 (light gray).

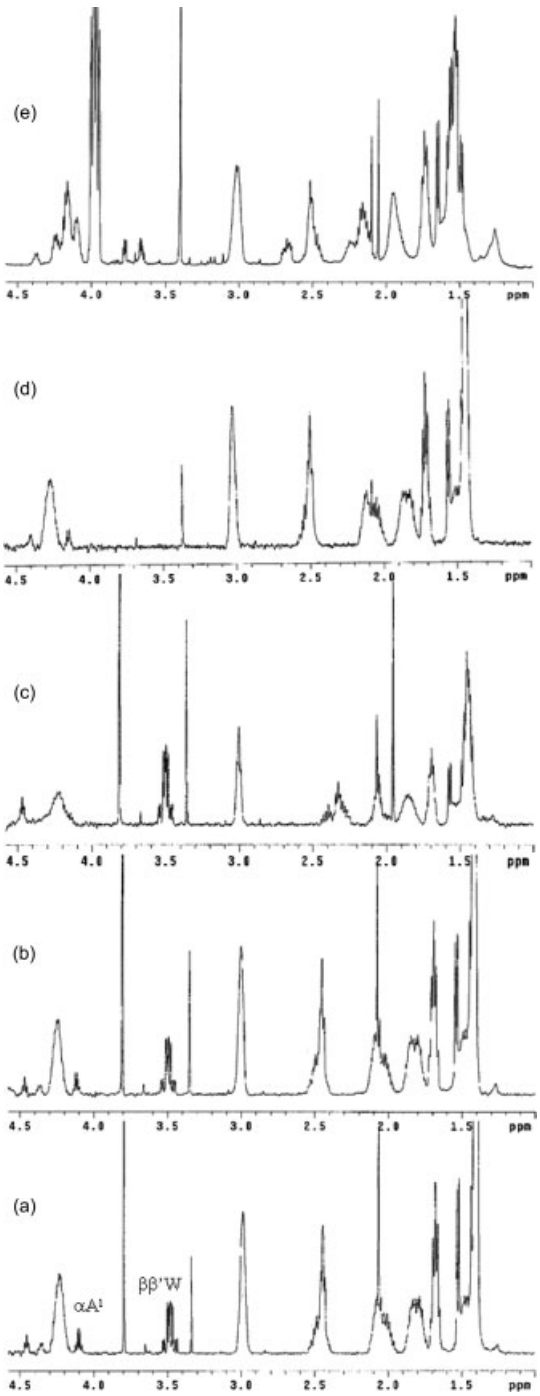


**Figure 2.** High-field regions of 1D NMR spectra of EAK16 in $H_2O/D_2O$ 90 : 10 v : v at 298 K: (a) freshly dissolved, $C_{peptide} = 0.95$ mM, $C_{Trp} = 0.78$ mM, pH = 3.27, no salt; (b) 5 months later; (c) pH raised to 5.13; (d) $C_{peptide} =$ 1 mM, $[Na^+] = 87$ mM, 3 months after the metal ion additions; (e) EAK16 1 mM in TFE/$H_2O$ 30/70 v : v.

  

we observe a negligible loss of the EAK16 spectral intensity (lower than 10%, in the limits of the measurement uncertainty). However, more interesting for the following discussion, the rate of the NMR visible peptide in solution measured at 'zero time' is less than 60% of the peptide amount put in solution.

*pH effect*

The spectral intensity loss observed at higher pH values (5.2–5.7) for EAK16 (Figure 2(c)), RGD-EAK16 and EYK16 suggests that neutral conditions favor self-aggregation phenomena. The intensity spectral reduction, in some cases coupled to the appearance of bumps in the baseline of the spectra, was not associated to perceptible precipitation events.

*Peptide concentration effect*

For all peptides of the 16-mer series, a peptide concentration increase in water from 0.5 to about 3 mM does not produce significant spectral variations (data not shown). In particular, no line broadenings are observed. It does mean that, were the self-aggregation processes active, these processes are irreversible or very slow on the NMR time scale.

*Metal ion effect*

The influence of sodium ion on the spectral behavior of the prototype EAK-16 was checked in two ways: (i) by progressive additions of micro volumes of concentrated NaCl (0.2 M in water) to the peptide sample ([$Na^+$] up to 100 mM) and (ii) by dissolving the peptide in water at salt concentration of 30 and 100 mM. With both the procedures no chemical shift changes or significant line broadening were observed (Figure 2(d)). However, in the presence of metal ions, the NMR spectrum of the sequence survives for shorter times. This is interpreted by considering that metal ions favor self-aggregation and that the aggregates, thus produced, are too large to be NMR detectable.

*Solvent effect*

The conformational behaviors of two sequences with high aggregation propensities, i.e. EAbuK16 and EAK16, and of the sequence RGD-EAK16-Sc were also tested in TFE/water mixture (30/70 v : v). In that *medium*, the peptides adopt a quite ordered structure. In the following, we just comment on EAK16, the prototype of the 16-mer series. The 1D spectrum of the peptide in TFE/$H_2$0 30/70 (v : v) is reported in Figure 2(e). The negative deviations from random coil values $\leq -0.1$ ppm measured for several $\alpha$CH residues (Figure 3) point to a helical conformation in the middle region of the peptide [28]. This structural diagnosis is consistent with the NOE pattern and $^3J_{NH-\alpha CH}$ coupling constants (Fig. S3 and Table S1 of the Supporting Information). Indeed, the observation of several unambiguous $NH_i - NH_{i+1}$ NOE effects more intense than the sequential $\alpha CH_i - NH_{i+1}$ contacts, suggest the presence of some ordered secondary structure. Furthermore, several long-range NOEs of the type $\alpha CH_i - \beta CH_{i+3}$ confirm the presence of a helical conformation in the middle region of the peptide. The molecular models obtained by DYANA/AMBER calculations (Figure 4) show that the peptide adopts an ordered structure with a backbone mean global RMSD of 1.26 ± 0.48 Å. The most ordered region of the peptide corresponds to the segment $A^3 - A^{13}$ where the backbone mean global RMSD for the superposition of the final ten structures is 0.27 ± 0.07 Å This region appears arranged in an $\alpha$-helical structure. Structure statistics are reported in Supporting Information (Table S2 and Fig. S4).

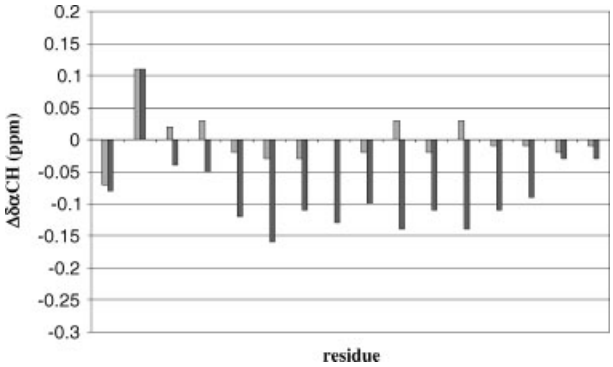


**Figure 3.** Chemical shift deviations from random coil values of $\alpha$CH protons ($\Delta\delta_{\alpha CH}$) of EAK16 1 mM in water (light gray) and in TFE/water 30/70 (v : v) (dark gray).

## Diffusion Measurements

In order to determine the aggregation state of the NMR visible molecular systems, PFGNMR experiments were performed on 1 mM-EAK16 sample in $H_2O/D_2O$ 90/10, pH 3.3 at 25 °C (Figure 5) and on 1 mM EAK16 sample in TFE/$H_2O$ 30/70, at 25 °C. The translational diffusion coefficients, $D_t$, obtained from fitting Eqn (1) (see Section on Material and Methods) to the peak intensities correspond to values of $(1.94 \pm 0.01) \times 10^{-10}$ $m^2$ $s^{-1}$ and $(1.37 \pm 0.01) \times 10^{-10}$ $m^2$ $s^{-1}$, respectively. The $D_t$ value obtained for EAK16 in $H_2O/D_2O$ 90/10 at higher concentration, 3 mM, was the same as the 1 mM-peptide within the limits of uncertainty. The apparent molecular mass estimated from diffusion coefficients (see Section on Material and Methods) showed EAK16 to be mostly in a monomeric form in all these conditions.

## Small Angle Neutron Scattering Study

Figure 6 reports the absolute scattering cross sections obtained for binary samples of EAK16 in $D_2O$ at acidic pH in the presence and in the absence of NaCl, and in a buffered solution at pH 6.8. An aqueous system containing the EAbuK16 has also been investigated and displayed in the same figure (acidic pH). To allow for an easy understanding of the results, data have been multiplied for a scale factor, as indicated.

Inspection of the figure allows concluding that cross sections scale with a power law $d\Sigma/d\Omega \propto q^{-1}$ typical of elongated structures, i.e. cylinders, rods, fibrils, etc. This is also in agreement with what found by Chen and coworkers [8].

A change of slope in the scattering cross sections is observed in the intermediate $q$ range. Such breakpoint is observed at $q \cong 2\pi/d$, where $d$ is the cross section length of the elongated scattering structures. From Figure 6 it is easy to observe that this region falls at the same values of $q$ ($\sim 5 \div 6 \times 10^{-2}$ $Å^{-1}$) for all systems but the one containing EAK16 at buffered pH. To get more precise quantitative information, scattering data have been analyzed to extract the cross diameter $d$ of these structures. Where the $q^{-1}$ regime holds, scattering cross sections are correlated with $d$ through [29]

$$\ln\left(q\frac{d\Sigma}{d\Omega}\right) = \ln[\phi(1-\phi)\pi\frac{d^2}{4}\Delta^2\rho] - q^2d^2 \qquad (2)$$

where $\phi$ is the volume fraction of the aggregates and $\Delta\rho$ represents the scattering density length difference existing between the scattering structures and the solvent ($D_2O$).



  

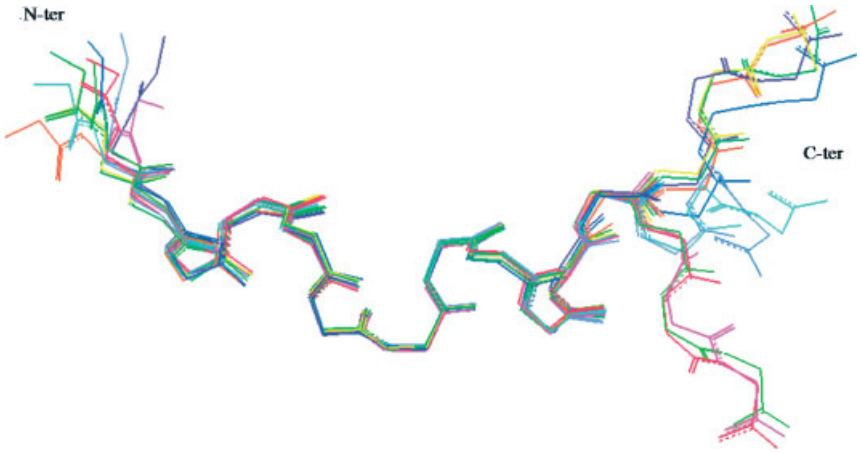


**Figure 4.** Molecular models of EAK16 1 mM in TFE/water 30/70 (v : v) calculated by the DYANA program: ensemble of the best ten structures after AMBER minimizations.

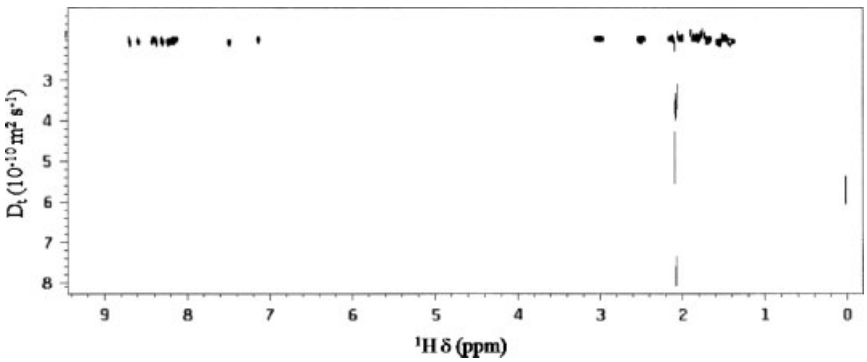


**Figure 5.** Diffusion coefficient of EAK16 1 mM in $H_2O/D_2O$ 90/10 (v : v), $D_t = (1.94 \pm 0.01) \times 10^{-10}$ m$^2$ s$^{-1}$.

From a fitting of the above equation, an inset of which is reported in Figure 6, the *d* values have been obtained and they are reported in Table 3. It is important to highlight that the missing of the Guinier regime for all the systems, does not allow evaluating the linear dimension *l* of the aggregates; this parameter must be greater than $2\pi/q_{min}$ where $q_{min}$ is the smallest *q* value attained with the SANS spectrometer (i.e. $l > 10^3$ Å).

Inspection of results of fittings reported in Table 3 confirms the qualitative features already inferred from the analysis of the data. A value of $d = 60 \pm 6$ is found for the EAK16 and EAbuK16 binary systems, and allows concluding that the replacement of the alanine with the $\alpha$-aminobutyric acid does not influence the packing of the molecules inside the aggregates.

The same value for *d* is found in the presence of NaCl, at least for the EAK16 system this could be ascribed to scarce influence of the salt on the net charge of the aggregates. On the other hand, when the pH value is raised from ≅3.3 (the pH of solutions obtained for simple dissolution of the solutes in water) to 6.8, a larger value of *d* is observed. This reflects, probably, the enhanced tendency to self-aggregation due to the partial molecules discharging, so that the hydrophobic effect dominates.

## Results: 8-Mer Analogs

The relevance of the peptide length in the aggregation process was checked through a structural characterization of the 8-mer analogs. The CD analyses suggest the peptides to be in a random conformation (Figure 7). CD results are consistent with the NMR analysis. The peptides are mainly in a disordered state although a slight tendency to adopt an extended structure is shown by their $\alpha$CH chemical shift deviations from the random coil values ($\Delta\delta_{\alpha CH}$) [28]. With the exception of EYK8, for which ring current effects are expected to be operative, all the sequences show positive $\Delta\delta_{\alpha CH}$ values (although below the threshold of 0.1 ppm) (Figure 8). A ROE pattern characterized by $\alpha CH_i - NH_{i+1}$ contacts more intense than the corresponding $\alpha CH_i - NH_i$ ones is measured for EAbuK8. Vice versa, $\alpha CH_i - NH_i$ ROE contacts more intense than the $\alpha CH_i - NH_i$ sequential effects, observed for DAOrn8, point to a definitively disordered state of the least hydrophobic peptide of the series. The molecular models calculated for EAbuK8 in water from experimental ROE restraints (see Fig. S5 of the Supporting Information) and by using DYANA program, confirm some propensities to the extended conformation. The ensemble of the best ten structures calculated for EAbuK8 in water is reported in Figure 9(a). The most ordered region of the peptide corresponds to the segment 3–6, where the backbone mean global RMSD for the superposition of the ten structures is 1.1 ± 0.6 Å. Finally, also the analog-bearing aromatic residues, EYK8, exhibits a number of ROEs (Fig. S5 of the Supporting Information) which allowed the calculation of a molecular model by DYANA program. The ensemble of the best ten structures calculated for EYK8 in water is reported in Figure 9(b). Most residues show $\phi$ and $\psi$ dihedral angles whose values land on the $\beta$-region of the Ramachandran plot (Fig. S6 of the Supporting Information). The most ordered region of the peptide corresponds to the segment 3–6, where

  

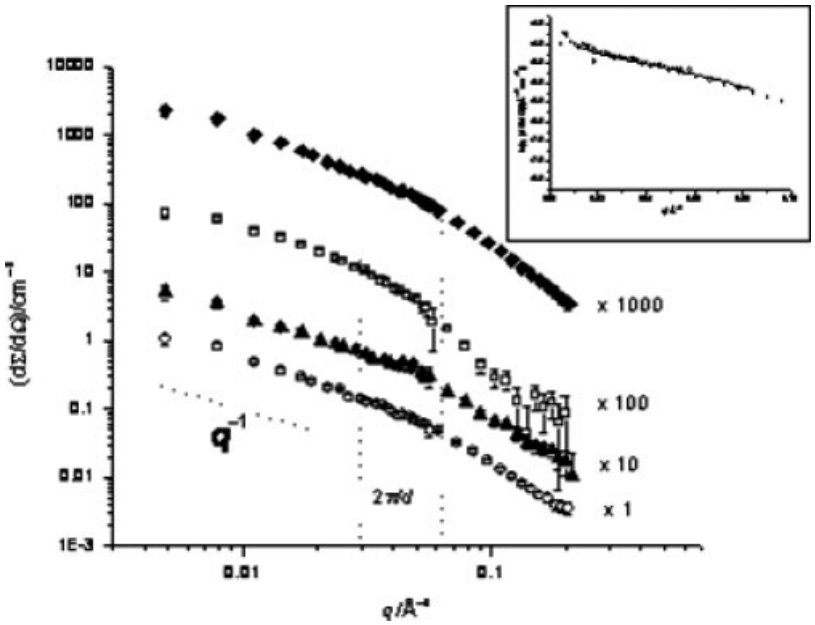


**Figure 6.** Scattering cross sections obtained at 25 °C for the following systems: ○ EAK16 (2.87 mM)/$D_2O$, pH ∼ 3.3
▲ EAK16 (1.02 mM)/NaCl (87 mM)/$D_2O$, pH ∼ 3.3
□ EAK16 (9.70 mM)/$D_2O$, pH 6.8
♦ EAbuK16 (3.32 mM)/$D_2O$, pH ∼ 3.3
To allow for an easy inspection, cross sections have been multiplied for a scale factor as indicated. The inset shows an example of fitting Eqn (2) to the experimental data, in order to calculate the structural parameters reported in Table 3.

**Table 3.** Diameters of the aggregates obtained through a fitting of Eqn (2) to the SANS experimental cross sections

| System | *d*/Å |
|---|---|
| EAK16 (3 mM)/$D_2O$ pH ∼ 3.3 | 60 ± 6 |
| EAK16 (1 mM)/NaCl (85 mM)/$D_2O$ pH ∼ 3.3 | 60 ± 6 |
| EAK16 (1 mM)/$D_2O$ pH 6.8 | 84 ± 8 |
| EAbuK 16 (3 mM)/$D_2O$ pH ∼ 3.3 | 60 ± 6 |

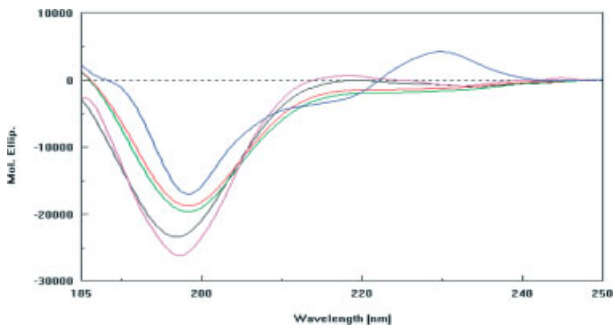


**Figure 7.** CD spectra of the 8-mer peptides 1 mM in water: EAK8 (black), DAK8 (red), DAOrn8 (green), EAbuK8 (fuchsia), EYK8 (blue).

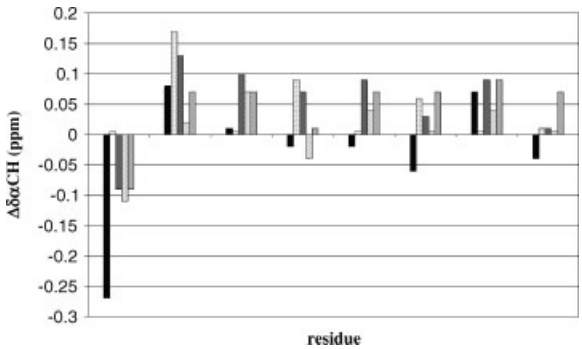


**Figure 8.** Chemical shift deviations from random coil values of αCH protons of the 8-mer analogs 1 mM in water: EYK8 (black), EAbuK8 (dotted), EAK8 (dark gray), DAK8 (dashed), DAOrn8 (light gray).

the backbone mean global RMSD for the superposition of the ten structures is 0.9 ± 0.6 Å. Structural statistics are reported in Table S3 of the Supporting Information.

The conformational behavior of the 8-mer analogs was checked at different values of concentration, pH, metal ions and hydrophobicity of the solvent and observed during time. However, in no conditions the 8-mer sequences clearly evidenced self-aggregating properties. Neither conformational transitions nor spectral intensity loss were observed with time or by changing the pH, or by adding salts. Peptide EAK8, as prototype of the series, was also studied in TFE/$H_2O$ 30/70 (v : v). In that media, the peptide is more ordered as shown by the higher αCH deviations from random coil values and the larger number of NOEs (data not shown).

### Diffusion Measurements

The translational diffusion coefficients obtained by PFGNMR experiments performed on 1 mM samples EAK8 in both $H_2O/D_2O$ 90/10 (v : v) and TFE/water 30/70 mixture at 25 °C ($D_t$ = (2.81 ± 0.01) × $10^{-10}$ $m^2$ $s^{-1}$ and (1.76 ± 0.01) × $10^{-10}$ $m^2$ $s^{-1}$ respectively), as well as for EYK8 1 mM in $H_2O/D_2O$ 90/10 ($D_t$ = (2.63 ± 0.01) × $10^{-10}$ $m^2$ $s^{-1}$) confirm that in the explored solvents the molecules are mostly in a monomeric state.

  

Journal of PeptideScience

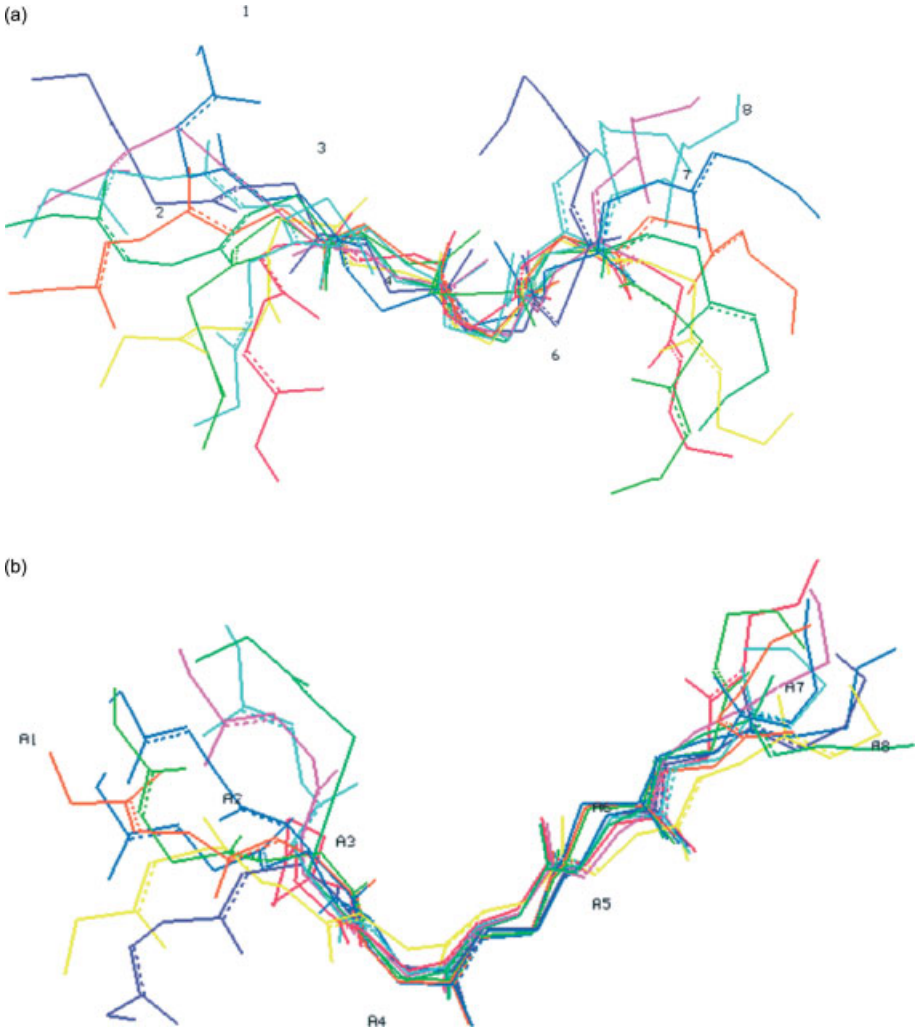


**Figure 9.** Molecular models of EAbuK8 and EYK8 (1 mM in water) calculated by the DYANA program: (a) ensemble of the best ten EAbuK8 structures; (b) ensemble of the best ten EYK8 structures.

### SANS Measurements

Differently from the corresponding 16-mer systems, the 8-mer systems we tested by SANS show cross section lower and more spread, indicating a scarce tendency to aggregation. Uncertainties associated to the cross section do not allow a reliable estimation of the transversal diameter of the scattering structures.

## Discussion and Conclusion

In this paper, the aggregative behavior of a series of ionic-complementary self-assembling peptides has been investigated by means of CD and NMR conformational analyses, translational diffusion coefficient measurements by PFGNMR and SANS experiments. The objective was to study the aggregation mechanism and specifically the role of hydrophobic and hydrophilic factors in the self-assembly process by comparing the behavior of the parent peptide, EAK16-II, with a series of analogs designed to have the same hydrophobic/negatively-charged/hydrophobic/positively-charged pattern but different residues.

The structural characterization of the self-complementary 16-mer and 8-mer analogs has shown that the higher propensities for self-aggregation in solution are exhibited by the longer and more hydrophobic sequences. Within the 8-mer series, a higher hydrophobicity correlates with higher propensity toward the extended conformation, the basic structural element for the $\beta$-sheet assembling. The molecular models obtained by ROE data for EAbuK8 and EYK8 in water shows that the peptides adopt a quite extended conformation with two well-defined aromatic and hydrophilic surfaces. However, at the explored solvent conditions, no 8-mer analogs give hints of self-aggregation.

In contrast, in mild conditions, i.e. at acidic pH and without salts, the most hydrophobic sequences in the 16-mer series, EYK16, EAbuK16, EAK16 and RGD-EAK16 are indeed involved in self-aggregation. While EYK16 self-assembles in weeks, the other sequences self-assemble very quickly but in different ratios. EAbuK16 has the highest propensity to form aggregates followed by peptide EAK16 and RGD-EAK16. It is worth noting that, for these sequences, the CD [9] and NMR analyses, taken separately, may drive to very different conformational diagnoses. The peptides EAbuK16, EAK16 and RGD-EAK16 all show CD profiles typical for $\beta$-structure. The same systems, with the exception of EAbuK16 (too self-aggregated to be NMR analyzed), are mainly random by NMR (5th column of Table 1). These apparent differences were interpreted by assuming that these sequences with high



  

$\beta$-propensities are distributed, in mild condition, between light (NMR visible) and heavy (CD visible) forms. For EAbuK16, this molecular distribution is significantly shifted toward heavy forms. Light forms are instead more abundant for EAK16 and RGD-EAK16. For EAK16, PFGNMR diffusion measurements and NMR characterization suggest that the light form is mainly due to monomers in random conformation. However, as qualitatively estimated by using an internal reference, not all the peptide molecules in solution give rise to the NMR spectra. The invisible part, i.e. the heavy form, corresponds to soluble aggregates with nuclear relaxation rates too high to be detected by NMR; in this respect, SANS measurements performed for EAbuK16 and EAK16 in water, confirm the presence in solution of soluble elongated aggregates with values of cross diameters of $\sim$60 Å. It is very possible that the floating objects revealed by SANS correspond to the CD-detected $\beta$-structured systems.

The molecular distributions of EAbuK16, EAK16 and RGD-EAK16 are very stable in time. The presence of NaCl, less acidic pH values and larger peptide concentrations promote aggregations. Two sequences of our series, DAK16 and DAOrn16, fail to adopt $\beta$-structure and do not show, at the explored conditions for the NMR analysis, self-assembling properties. The data are surprising because peptides DAK16 and DAOrn16 preserve the beta-sheet periodicity of the prototype EAK16. The modification introduced in the two analogs involves the charged residues and not the hydrophobic ones, as in the EAbuK16 case. In our opinion, in disagreement with the hypothesis formulated by Xiong and Zhang, the beta-sheet periodicity is a very important determinant but it is not the only one. Although DAK16 shows the same mean hydrophobicity moment of EAK16, it fails to arrange into a beta structure. This result implies a role also of the hydrophilic sequence of the peptide in the assembly and it specifically appears that shorter side chains of acid residues are able to impair $\beta$-sheet formation.

With the aim to characterize soluble aggregates by NMR, we tried to tune the self-assembling ability of EAbuK16 and EAK16 by using a solvent with a reduced hydrophilicity. Once again the structural diagnosis from NMR was different from the CD one. While CD analysis shows that the peptides are mainly involved in $\beta$-structure [9], NMR techniques just read conformational components of helix type. In the case of EAK16, diffusion measurements also proved that the NMR visible structure is in a monomeric state. On the basis of a comparison between CD and NMR/PFGNMR results and considering the analogy with the behavior of the peptides in water, we propose that even when dissolved in TFE/$H_2O$ 30/70 (v : v), these sequences are distributed between heavy and light forms.

The structural knowledge of the self-assembled products is a fundamental step for designing aggregates with specific properties and functions. Details on aggregation mechanisms may be caught by stabilizing and characterizing early soluble aggregates. However, this aim is quite critical to fix, as the extensive studies on amyloidosis mechanisms show. This study, on synthetic amphiphilic peptides, confirms these difficulties. Even in mild condition, the soluble aggregates are too large to be investigated by NMR. In agreement with Fung *et al*. [8], our results, obtained by analyzing the sequences in solution, suggest that the mechanisms of self-assembling for this class of molecules proceed by nucleation.

Finally, as *a latere* issue, we note that peptides designed to adopt $\beta$-structure can fold, in an appropriate *medium*, in helix structure. Similar results were observed by Mutter *et al*. in their studies on amphiphilic 'switch peptides' in aqueous and TFE/water solutions [30,31]. We have shown that the ionic-complementary prototype EAK16 in TFE/water mixture (30/70 v:v) is distributed between helix monomers and $\beta$-aggregates. Interestingly, this structural conversion mimics $\beta$-amyloid peptide aggregation mechanisms.

### Supporting information

Supporting information may be found in the online version of this article.

### Acknowledgements

This work was supported by the grant PRIN-2005039419_003 from Ministero dell'Università e della Ricerca (MIUR) of Italy. The authors thank the Laboratoire Leon Brillouin for the provision of beam time.

## References

1. Zhang S, Altman M. Peptide self-assembly in functional polymer science and engineering. *React. Funct. Polym.* 1999; **41**: 91–102.
2. Chiti F, Dobson CM. Protein misfolding, functional amyloid, and human disease. *Annu. Rev. Biochem.* 2006; **75**: 333–366.
3. Zhang S. Fabrication of novel biomaterials trough molecular self-assembly. *Nat. Biotechnol.* 2003; **21**: 1171–1178.
4. Holmes TC. Novel Peptide-based biomaterial scaffolds for tissue engineering. *Trends Biotechnol.* 2002; **20**: 16–21.
5. Zhang S, Holmes T, Lockshin C, Rich A. Spontaneous assembly of a self-complementary oligopeptide to form as stable macroscopic membrane. *Proc. Natl. Acad. Sci. U.S.A.* 1993; **90**: 3334–3338.
6. Chen P. Self-assembly of ionic-complementary peptides: a physicochemical viewpoint. *Colloids Surf.* 2005; **261**: 3–24.
7. Xiong H, Buckwalter BL, Shieh HM, Hecht MH. Periodicity of polar and nonpolar amino acids is the major determinant of secondary structure in self-assembling oligomeric peptides. *Proc. Natl. Acad. Sci. U.S.A.* 1995; **92**: 6349–6353.
8. Fung SY, Keyes C, Duhamel J, Chen P. Concentration effect on the aggregation of a self-assembling oligopeptide. *Biophys. J.* 2003; **85**: 537–548.
9. Gambaretto R, Tonin L, Di Bello C, Dettin M. Self-assembling peptides: correlation among sequence, secondary structure in solution and film formation. *Biopolymers* 2008; **89**: 906–915.
10. Tinti A, Di Foggia M, Taddei P, Torreggiani A, Dettin M, Fagnano C. Vibrational study of auto-assembling oligopeptides for biomedical applications. *J. Raman Spectrosc.* 2008; **39**: 250–259.
11. Bax Ad, Davis DG. MLEV-17-based two-dimensional homonuclear magnetization transfer spectroscopy. *J. Magn. Reson.* 1985; **65**: 355–360.
12. Jeener J, Meier BH, Bachmann P, Ernst RR. Investigation of exchange processes by two-dimensional NMR spectroscopy. *J. Chem. Phys.* 1979; **71**: 4546–4553.
13. Kumar A, Wagner G, Ernst RR, Wüthrich K. Buildup rates of the nuclear Overhauser effect measured by two-dimensional proton magnetic resonance spectroscopy: implications for studies of protein conformation. *J. Am. Chem. Soc.* 1981; **103**: 3654–3658.
14. Bax Ad, Davis DG. Practical aspects of two-dimensional transverse NOE spectroscopy. *J. Magn. Reson.* 1985; **63**: 207–213.
15. Piantini U, Sørensen OW, Ernst RR. Multiple quantum filters for elucidating NMR coupling networks. *J. Am. Chem. Soc.* 1982; **104**: 6800–6801.
16. Wüthrich K. *NMR of Proteins and Nucleic Acids*. John Wiley and Sons: New York, 1986.
17. Johnson BA, Blevins RA. NMRView: a computer program for the visualization and analysis of NMR data. *J. Biomol. NMR* 1994; **4**: 603–614.
18. Guntert P, Mumenthaler C, Wüthrich K. Torsion angle dynamics for NMR structure calculation with the new program DYANA. *J. Mol. Biol.* 1997; **273**: 283–298.
19. Wüthrich K, Billeter M, Braun W. Pseudostructures for the 20 common amino acids for use in studies of protein conformations by

  

measurements of intramolecular proton-proton distance constraints with nuclear magnetic resonance. *J. Mol. Biol.* 1983; **169**: 949–961.
20. Karplus M. Vicinal proton coupling in nuclear magnetic resonance. *J. Am. Chem. Soc.* 1963; **85**: 2870–2871.
21. Guntert P, Wüthrich K. Improved efficiency of protein structure calculations from NMR data using the program DIANA with redundant dihedral angle constraints. *J. Biomol. NMR* 1991; **1**: 447–456.
22. Pearlman DA, Case DA, Caldwell JW, Ross WS, Cheatham TE III, DeBolt S, Ferguson D, Seibel G, Kollman P. AMBER, a package of computer programs for applying molecular mechanics, normal mode analysis, molecular dynamics and free energy calculations to stimulate the structural and energetic properties of molecules. *Comput. Phys. Commun.* 1995; **91**: 1–41.
23. Koradi R, Billeter M, Wüthrich K. MOLMOL: a program for display and analysis of macromolecular structures. *J. Mol. Graphics* 1996; **14**: 51–55, plates 29–32.
24. Wu D, Chen A, Johnson CS Jr. An improved diffusion-ordered spectroscopy experiment incorporating bipolar-gradient pulses. *J. Magn. Reson., Ser. A* 1995; **115**: 260–264.
25. Danielsson J, Jarvet J, Damberg P, Graslund A. Translational diffusion measured by PFG-NMR on full length and fragments of the Alzheimer A$\beta$(1–40) peptide. Determination of hydrodynamic radii of random coil peptides of varying length. *Magn. Reson. Chem.* 2002; **40**: S89–S97.
26. Wignall GD, Bates FS. Absolute calibration of small-angle neutron scattering data. *J. Appl. Crystallogr.* 1987; **20**: 28–40.
27. Russell TP, Lin JS, Spooner S, Wignall GD. Intercalibration of small-angle x-ray and neutron scattering data. *J. Appl. Crystallogr.* 1988; **21**: 629–638.
28. Wishart DS, Sykes BD, Richards FM. Relationship between nuclear magnetic resonance chemical shift and protein secondary structure. *J. Mol. Biol.* 1991; **222**: 311–333.
29. Radulescu A, Mathers RT, Coates GW, Richter D, Fetters LJ. A SANS study of the Self-assembly in solution of syndiotactic polypropylene homopolymers, syndiotactic polypropylene-block-poly(ethylene-co-propylene) diblock copolymers, and an alternating atactic-isotactic multisegment polypropylene. *Macromolecules* 2004; **37**: 6962–6971.
30. Mutter M, Hersperger R. Peptides as conformational switch: Medium-induced conformational transitions of designed peptides. *Angew. Chem., Int. Ed. Engl.* 1990; **29**: 185–186.
31. Mutter M, Gassmann R, Buttkus U, Altmann KH. Switch peptides: pH-induced $\alpha$-helix to $\beta$-sheet transitions of bis-amphiphilic oligopeptides. *Angew. Chem., Int. Ed. Engl.* 1991; **30**: 1514–1516.

  